Dawn-dusk Asymmetrical Distribution of Saturn's Cusp

Y. Xu[1,2], Z. H. Yao[2]*, C. S. Arridge[3], B. Zhang[2], J. J. Chen[2], S. V. Badman[3], L. C. Ray[3], A. J. Coates[4,5] ,S.-Y. Ye[1], T. S. Qin[2], Z. Q. Zheng[2,6], W. R. Dunn[4], Y. Wei[7]

[1] Department of Earth and Space Sciences, Southern University of Science and Technology (SUSTech), Shenzhen, China

[2] Department of Earth and Planetary Sciences, the University of Hong Kong, Pokfulam, Hong Kong SAR, China

[3] Department of Physics, Lancaster University, Lancaster, UK

[4] Mullard Space Science Laboratory, University College London, Dorking, UK

[5] Centre for Planetary Sciences at UCL-Birkbeck, London, UK

[6] Meta force Institute of Computation and Information Co Limited, Hong Kong SAR, China

[7] Institute of Geology and Geophysics, Chinese Academy of Sciences, Beijing, China

Correspondence and requests for materials should be addressed to Zhonghua Yao (yaozh@hku.hk)

Abstract

Saturn's magnetosphere, shaped by solar wind interaction with its dipole field, differs from Earth's due to faster rotation and Enceladus's internal plasma sources. An ongoing focus of investigation is how the internal plasma sources and rapid rotation result in a different global magnetospheric picture. The magnetospheric cusp, a crucial interaction region between solar wind and planetary magnetic field, serves as an indicator of global magnetic configuration. Here we utilize Cassini observations from 2004 to 2010 to study dawn-dusk asymmetry in Saturn's cusp distribution and extend the number of cusp events from about 11 reported in previous studies to 67. We find peak occurrence in the post-noon sector and signatures extending to post-dusk (near 20 local time), resembling recent observations of Jupiter's post-dusk cusp. We further examine magnetic topology using high-resolution magnetohydrodynamic simulations to visualize the cusp asymmetry. This is consistent with previous studies but our simulations provide a more detailed view of Saturn’s magnetic topology near the magnetopause. This asymmetry of cusp distribution demonstrates how rapid rotation and internal plasma sources fundamentally alter magnetospheric configuration, offering insights for understanding other rotating planetary systems within and beyond the solar system.

Introduction

Planetary magnetospheres are formed as a result of the continuous interaction between the high-speed solar wind and the internally generated magnetic fields present in most planets within the solar system, which display considerable variations among different planets. For example, the magnetospheres of Jupiter and Saturn are more internally driven because of the planets' rapid rotation speeds coupled with internal plasma sources within their magnetospheres, which differs

from the strongly solar wind-driven magnetospheres typically seen on Earth[1,2]; In the case of ice giants like Uranus and Neptune, the unique pole-on configuration of their magnetospheres – the geometry in which the upstream solar-wind flow is approximately aligned with the planet's magnetic dipole axis – leads to distinct coupling dynamics with the solar wind[3,4]. At the same time, the highly dynamic nature of these gas giants' plasma environment fosters complex interactions with the solar wind which contributes as an external factor to the magnetospheric dynamics[5,6]. Understanding these diverse magnetospheric dynamics can help improve the interpretation of observations of planetary systems and offer useful perspectives for the broad field of planetary science, such as star-planet interactions.

When the solar wind interacts with a planetary magnetosphere, magnetic reconnection on the magnetopause often occurs where the magnetic shear is sufficiently large. At Earth, magnetopause reconnection is strongly governed by the north–south component of the interplanetary magnetic field (IMF)—with southward IMF driving subsolar reconnection and northward IMF favoring high-latitude lobe reconnection[7]. In the rotationally dominated magnetospheres of giant planets, magnetopause reconnection was reported to be favored at high latitudes. In contrast, low-latitude subsolar reconnection is often suppressed by diamagnetic effects and is therefore less likely to occur there[8–10]. Recent simulations[11–13] have suggested that reconnection at Jupiter is strongly influenced by the east–west IMF component, with reconnection occurring predominantly at high latitudes and suppressed reconnection at low-latitude magnetopause locations. During reconnection, solar wind particles are allowed to enter the magnetosphere through the newly reconnected magnetic field lines. The magnetospheric cusp is known as a vital funnel-shaped region that permits these particles to directly access the atmosphere[14,15]. The cusps play a crucial role in planetary magnetospheres, as they significantly

contribute to various mass and energy transport processes within the magnetosphere, ionosphere, and upper atmosphere. These processes are key in the formation of geomagnetic storms[16], sub-storms[17], and auroras[18]. A series of in situ studies, e.g., using the Cluster multi-spacecraft mission, have revealed that Earth's cusp is a broad, complex region characterized by various intriguing boundary layers[14,19]. The cusp in Earth's quiescent magnetosphere, strongly governed by solar wind, typically exhibits a general morning-afternoon symmetry of its morphology and statistical occurance rates, which is one of the most fundamental properties of terrestrial cusp[20,21]. although the distribution of its spatial location can be influenced by the IMF B_y component and pressure of the solar wind[22,23]. In contrast, due to Saturn's rapid rotation, the Kronian magnetospheric plasma generally subcorotates relative to the planet, remaining in near-rigid corotation within approximately 20 R_S, but falling significantly below the rigid corotation rate beyond Titan's orbit[24,25]. Compared to Earth, Jupiter exhibits bright and persistent polar auroras[26], and Saturn's aurora shows variable morphologies resembling both Earth-like and Jupiter-like structures[27], suggesting a markedly different magnetospheric configuration and dynamics of rapid-rotating giant planets[2,28,29]. The rapid rotation of giant planets plays a crucial role in modifying magnetic flux transport within the magnetosphere and near the magnetopause compared to Earth[12,29]. This rotational influence can modify dawnside magnetopause reconnection rates associated with solar wind interaction and alter the configuration of the magnetopause and the open–closed field line boundary, where the cusps are anchored[12,29].

Zhang et al.[11,29] provide additional insights into the distinct magnetospheric configurations of Earth and giant planets using high-resolution simulations. In rotation-dominated Jovian-like systems, low reconnection rates on the dawn side can cause closed flux to accumulate there, resulting in an open flux fraction of approximately 20% in the polar region (above 80° magnetic

latitude, MLAT[20]). Conversely, terrestrial-like magnetosphere is mostly solar wind-dominated exhibiting near-complete openness of the polar region above 80° MLAT (about 98%)[29]. Although Saturn's magnetosphere is similarly rotation-dominated, its weak magnetic field (0.21 G of equatorial magnetic field strength, about 1/20 of Jupiter's[30]) results in its reduced corotation dominance. The consequently higher solar wind merging potential-to-corotation potential ratio (0.38 at Saturn vs. 0.09 at Jupiter[29]) increases solar wind-driven flux opening efficiency. As a result, Kronian-like magnetosphere's polar open flux fraction varies widely (58–93% above 80° MLAT)[29]. Observationally, Saturn's high-latitude magnetosphere has been reported to be largely plasma-depleted and composed predominantly of open field lines, with the polar cap boundary located at $14.5 \pm 0.6°$ and $12.7 \pm 0.6°$ colatitude in the southern and northern hemispheres, respectively[31,32]. Comparing to Jupiter's small open flux area, Saturn's relatively large area of open magnetic field may result in a more observable cusp, although more detailed analysis and observations are needed to confirm the prediction. Previous theoretical models by Cowley et al. (2004, 2005)[33,34] proposed that rotational dynamics drive the subsolar X-line at Saturn, thereby influencing the azimuthal distribution of the polar cap and cusp in local time. This framework is based on terrestrial magnetopause reconnection pictures and the Dungey[7]/Vasyliūnas cycle[35]. But the applicability of the Dungey cycle to giant planets remains a topic of active debate[36].

Currently, the global distribution picture of Saturn's cusp remains an active topic of ongoing research. As shown in simple schematic Fig. 1, a comparative analysis of Saturn's cusp distribution with Earth's is crucial for understanding the diverse planetary magnetospheres and their interaction with the solar wind.

Some case studies have identified characteristics in Saturn's cusp region, such as magnetosheath-like electron features and ion dispersion patterns that are similar to those observed in Earth's cusp[37–40]. Additionally, variations in ion dispersion features under different reconnection conditions and magnetic depression features in Saturn's cusp have been examined, revealing parallels with Earth's cusp[37,38,40]. These similarities indicate that the microphysical processes governing the behavior of charged particles within cusps might be universal across different planetary environments. However, the study by Arridge et al.[40] noted cusp encounters recurring in sync with Saturn's rotation period, thought to be linked to the cusp position oscillating in phase with Saturn's global magnetospheric dynamics[40]. Previous researches utilizing global magnetohydrodynamic (MHD) simulations have demonstrated that the magnetospheric structure of rapidly rotating giant planets exhibit significant asymmetries[41], markedly different from those observed at Earth[11,12]. For instance, simulation studies have shown that rapid rotation significantly alters the global magnetospheric configuration of Jupiter, notably causing a pronounced duskward shift in the open magnetic field regions associated with Jupiter's polar cusp[11,12]. This dusk-side distribution of Jupiter's cusp has been supported by observational results from Xu et al. (2024)[13]. Given Saturn's rotation-dominated magnetosphere, a similar duskward shift in its cusp distribution is expected[13,29].

However, several questions remain unresolved. A comprehensive global observational picture of cusp regions at giant planets is still lacking. At Jupiter, due to Juno's current orbital constraints[13,42,43], high-latitude observations in the middle-to-outer magnetosphere across various local times remain incomplete, leaving the properties and distribution of cusp regions in the dawn, noon, and post-noon sectors mysterious. Given Saturn's similarly rapidly rotating magnetosphere, investigating its global cusp distribution is especially important. Such research

provides valuable comparative insight into Jupiter's reported dusk-side cusp and informs future observations of Jupiter's cusp and high-latitude boundary layer regions. Previous studies have provided valuable analyses of several Saturn cusp events[37–40]. Here we extend this foundation by offering a global, dwell-time–normalized statistical view, enabling an global assessment of the cusp occurrence distribution.

In the present research, we explored the global distribution of Saturn's cusp using data from the Cassini spacecraft, spanning from 2004 to 2010. Additionally, we employed high-resolution MHD simulations[11,12,44] to visualize the magnetic configurations of Saturn and its cusp, revealing Saturn's magnetopause related three-dimensional magnetic topology. Both the statistical analysis and the simulation results highlight the characteristics of the morning-afternoon asymmetry in Saturn's cusp, which diverges from the symmetric distribution observed at Earth and shows consistency with Jupiter's recently discovered configuration.

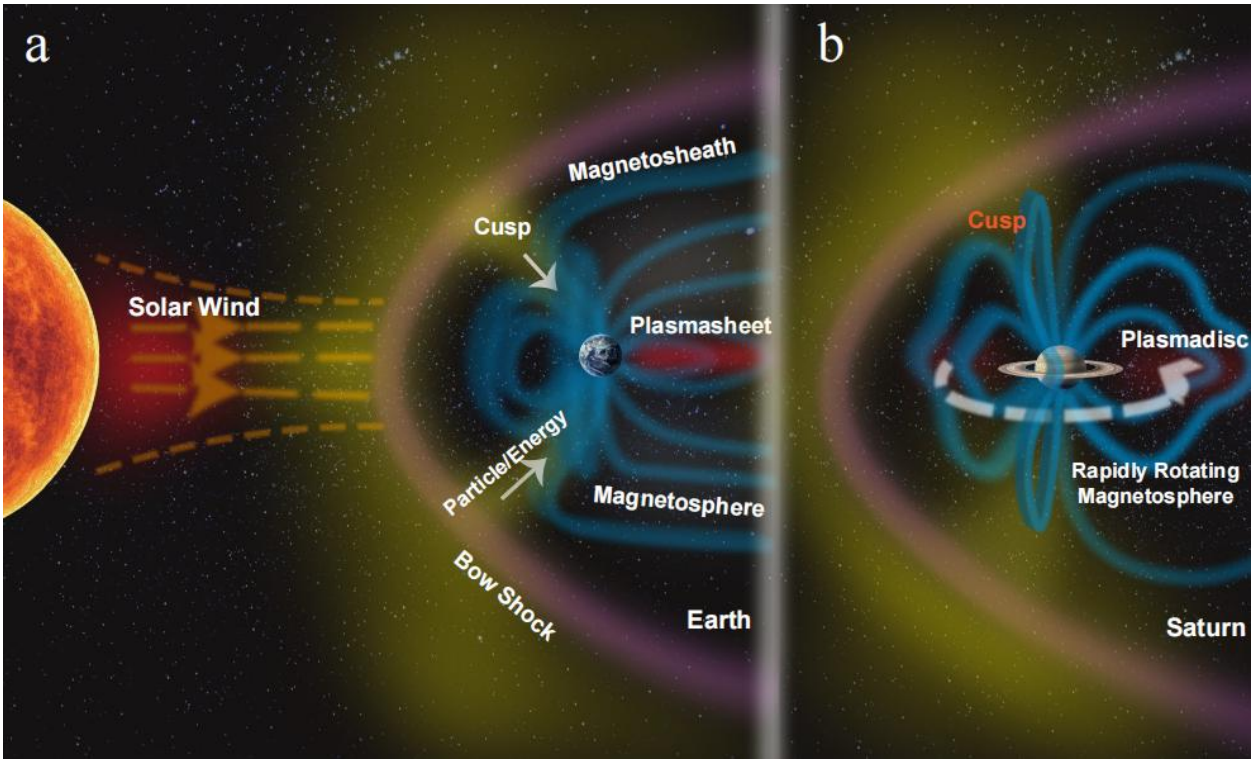

Figure 1. A simple schematic of the configuration of the solar wind-driven Earth magnetosphere and the rapidly rotating Saturn magnetosphere. (**a**) Schematic of Earth's magnetosphere configuration showing the noon-centered cusp distribution. The cusp is located generally around local noon where solar wind particles can enter; (**b**) Schematic of Saturn's rapidly rotating magnetosphere. illustrating the incompletely understood global cusp distribution investigated in this study. The full extent of the global cusp distribution at Saturn remained uncompletely clear prior to this work. Noted that Figure 1 might not be appropriate for Jupiter[29].

Results

Kronian cusp observation case. A Kronian cusp case is presented for the period between 23:00 on January 30 and 05:00 on January 31, 2009, when the Cassini spacecraft was located in the high latitude (>40°) noon region of the northern hemisphere, near 16 R_s (Fig. 2). Cassini transitioned from the magnetospheric region to the boundary layer and the cusp region, as shown in Fig. 2. In this study, we examine Cassini's in-situ measurements from three key sources: the Cassini Magnetometer instrument (MAG)[45], Cassini Plasma Spectrometer - Electron Spectrometer (CAPS-ELS)[46], and Cassini Plasma Spectrometer - Ion Mass Spectrometer (CAPS-IMS)[46]. Before 23:51 UT, as indicated by the first dashed line in Fig. 2, Cassini recorded a magnetospheric electron spectrum with enhanced energy ranges between 1000 and 10000 eV. In this region, the ion energy spectrum displayed no distinct features, and the electron pitch angle distribution was isotropic. These characteristics are indicative of the magnetosphere at this location[30,40]; hence, this region is identified as part of the magnetosphere and is denoted by the letter M in Fig. 2. After 00:36 UT marked by the second dashed line in Fig. 2, the spacecraft

observed a region characterized by a notable enhancement in the electron energy spectrum from 10 to 100 eV, as depicted in Fig. 2c. This enhancement is characteristic of magnetosheath electrons[47]. Concurrently, the magnetic field component remained relatively stable as shown in Fig. 2a, b, which negates the likelihood of the spacecraft being in the magnetosheath. Additionally, observations included a bidirectional distribution of low-energy electrons and a rise in high-energy electrons opposing the magnetic field direction (shown in Fig. 2e, f, g, h), along with multiple ion dispersion signals. These observations suggest that the magnetopause experienced pulsed reconnection processes[37,48]. These distinct features robustly indicate that the region encountered by the spacecraft is indeed a magnetospheric cusp region[37,38,40]. Situated between the magnetosphere and the cusp is a transitional area, characterized by plasma properties that are intermediate between those of the magnetosphere and the cusp. This region is identified as a boundary layer and is denoted by BL in Fig. 2.

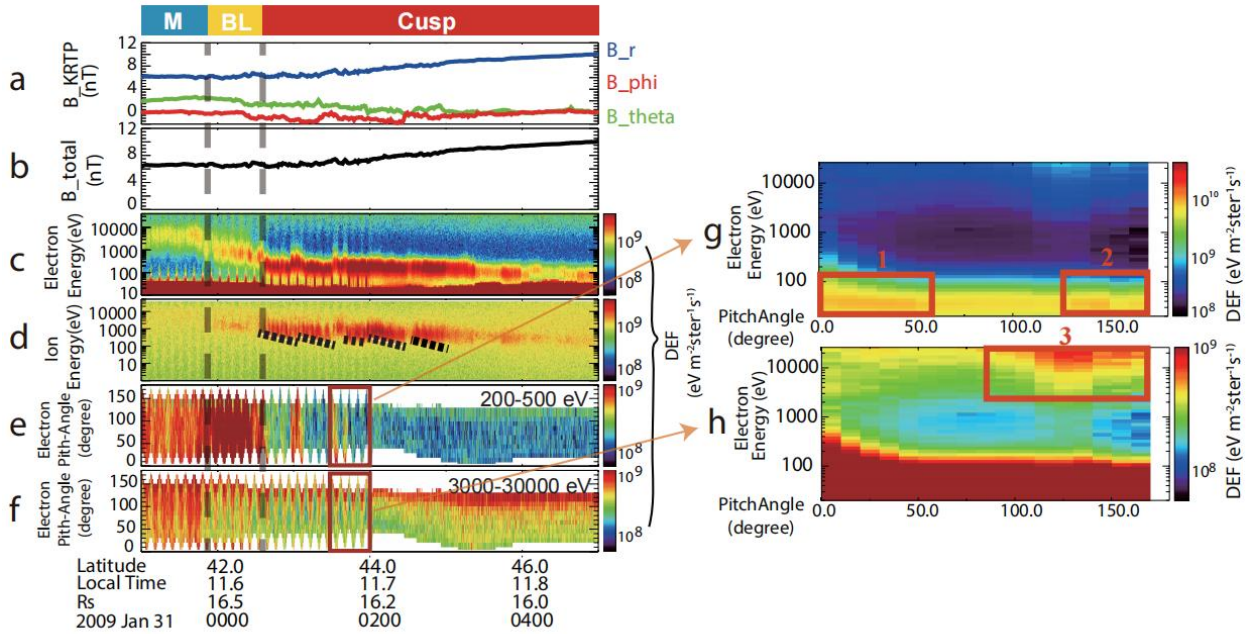

175

Figure 2. The Kronian cusp observations revealed by Cassini's MAG and CAPS instruments on January 31, 2009. (**a**) Three magnetic field components in Kronocentric-R-Theta-Phi (KRTP) coordinates. (**b**) The total magnetic field strength. (**c**) The electron energy spectrogram. (**d**) The ion energy spectrogram. (**f**) The ion energy spectrogram. (**e**)-(**f**) Pitch angle distribution for electrons within energy ranges of 200 eV to 500 eV and 3 keV to 30 keV. (**g**)-(**h**) Pitch angle distribution for electrons averaged between 01:30 to 02:00. Black dashed lines in panel d indicate the ion dispersion signatures in the cusp region. Boxes in panels e-h and numbers 1-3 represent the bidirectional distribution of low-energy electrons and high-energy electrons. Panel g-h refers to the specific averaged electron pitch angle distribution in different energy ranges from 01:30 to 02:00 as indicated by the boxes of panel e-f. The region is identified as part of the magnetosphere and is denoted by the letter M. This region is identified as a boundary layer and is denoted by BL.

Statistical investigations and MHD simulation results. To identify Kronian cusp events, the most important criteria, based on previous research on Saturn's cusp[37,38,40] and Jupiter's cusp[13], are as follows: (1) Spacecraft location, e.g., relatively high latitudes (>30 degrees) and within the magnetopause; (2) Most typical plasma characteristics within cusp regions, e.g., magnetosheath-like electron energy distributions[13,37,38,40]. These are referred to as the Level 1 criteria, which are the most critical for identification. Most Saturn cusp events can be well identified by meeting these criteria. Additionally, other important but non-essential features can further aid in identification, including ion dispersion[37,40] associated with magnetopause reconnection, field-aligned electron distributions[37,40], and magnetic depressions[39] within cusp regions. These are referred to as the Level 2 criteria, which can be helpful but not necessary for cusp identification.

Utilizing all these criteria, we identified a total of 67 cusp events that matched the characteristics observed by the Cassini spacecraft between 2004 and 2010. These events encompass previously reported cases of Saturn's cusp region, demonstrating the reliability of our identification and the consistency of this study with prior research. Information on Saturn's cusp events and the corresponding criteria fulfillment is organized in the Supplementary Data 1. It is noted that the survey period of 2004–2010 corresponds to the timeframe from Cassini's entry into Saturn's bow shock to the final year before the CAPS instrument was placed in Operations on Hold (2011)[38]. Since the detection of magnetosheath-like electron spectra by CAPS provides the most direct and essential evidence for cusp identification[14,20,40], data collected after 2011 were excluded to ensure the reliability of event identification. This study does not distinguish between cusp types associated with different magnetopause reconnection pictures. Recent findings suggest that magnetopause reconnection at giant planets may be significantly more complex than the subsolar/lobe-dominated patterns observed at Earth, with reconnection-related dynamics exhibiting greater variability[11–13]. Moreover, long-term, stable solar wind measurements are lacking at Saturn during the Cassini mission[39,40], and solar wind models cannot provide real-time, accurate information on the east–west and north–south components of IMF[39,40,49]. As a result, identifying cusp types based on ion dispersion signatures linked to specific reconnection geometries is highly challenging and beyond the scope of this study.

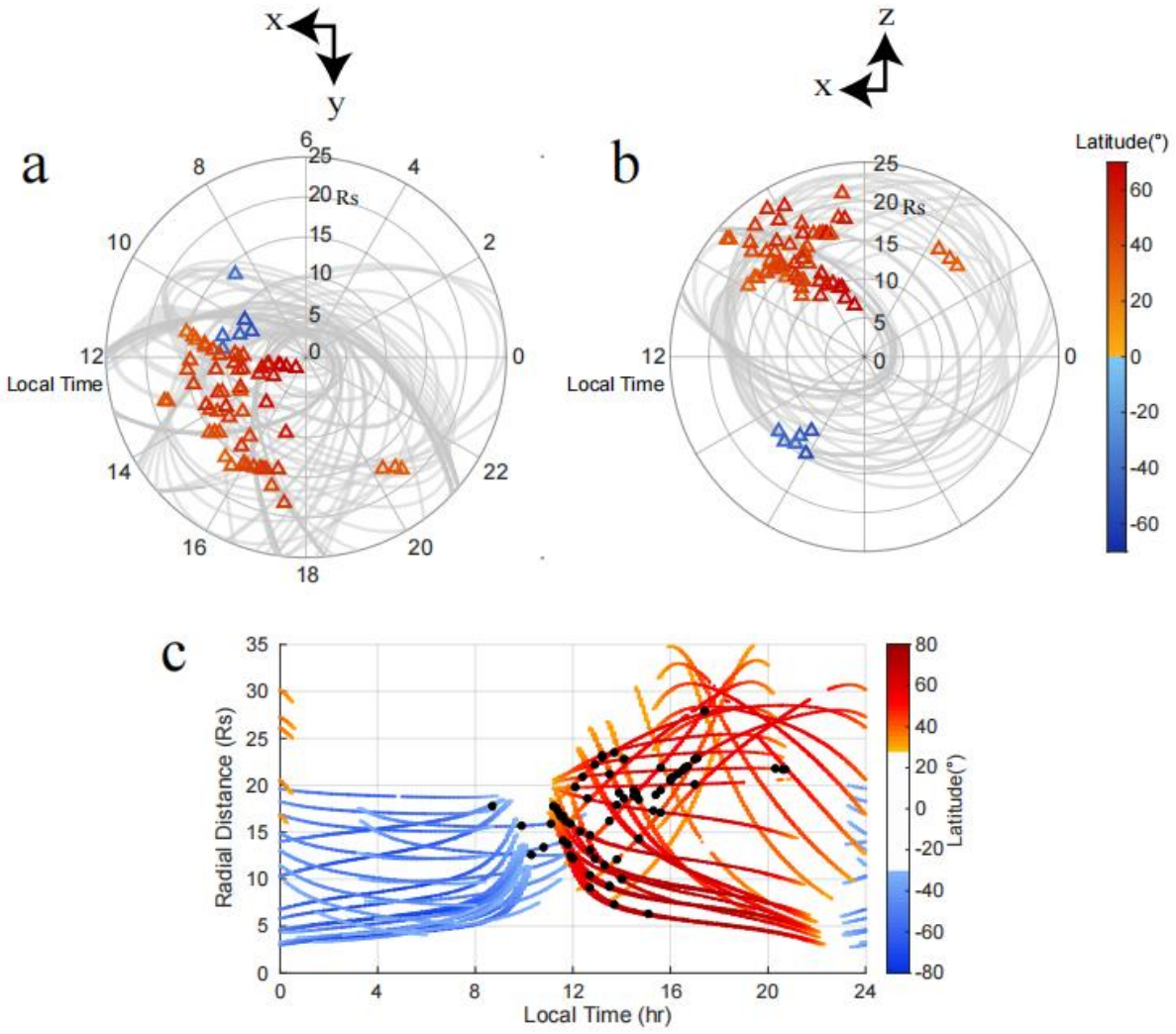

Figure 3. Statistical global distribution of 67 Kronian cusp events from the year 2004 to 2010. Global distribution of all cusp events in (**a**) X-Y view and (**b**) X-Z view of Kronocentric solar magnetospheric (KSM) coordinate, in which the trajectories of the spacecraft are superimposed. (**c**) The radial distribution of cusp events at different local times. Gray curves in panels a-b show Cassini spacecraft trajectories during the survey period. Black dots in panel c indicate the locations of identified cusp crossings. The trajectory of the spacecraft with latitude information is also superimposed in panel c. Red for the Northern Hemisphere, and blue for the Southern Hemisphere.

The global distribution of these events is presented in Fig. 3. Fig. 3a and 3b demonstrate that the majority of observed cusp events are located in the northern hemisphere and predominantly on the afternoon side, with some events even detectable on the post-dusk side (more than 20 local time, LT). Fig. 3c displays the distribution of cusp events at high latitudes (>30° or <-30°) across various radial distances and local times. Due to the Cassini spacecraft's trajectory constraints, its high-latitude path in the southern hemisphere is primarily on the morning side, while in the northern hemisphere, it's largely on the afternoon side. Notably, between radial distances of 10 and 20 R_s, high-latitude tracks are present on both the morning and afternoon sides. However, there is a marked contrast in event density for 10 to 20 R_s radial range in high latitudes (shown in Fig. 3c). Between 13 and 16 LT, a total of 17 cusp events were identified within Cassini's accumulated dwell time of 36,626 minutes, corresponding to an event density of approximately 0.028 events per hour. In contrast, during the interval from 8 to 11 LT with a dwell time of 37,379 minutes, only 4 cusp events were detected, indicating a substantially lower event density of 0.006 events/hour. Although previous studies have reported minor differences in the period of kilometric radiation waves north and south of Saturn[50,51], there is currently insufficient evidence to suggest a pronounced north-south asymmetry in Saturn's magnetospheric configuration that can notably impact the polar cusp structure. Thus, this study posits that the observed distribution reflects the morning and afternoon asymmetry in Saturn's cusp distribution. More importantly, three post-dusk cusp events were identified during the statistical study, with the specific identification criteria for each event detailed in Supplementary Data 1. And comprehensive plasma analyses, along with comparisons distinguishing these events from nightside ionospheric outflows, are provided in Supplementary Note 1 and Supplementary Figs. 1–3. The plasma

energy spectra and spatial distributions of these events closely resemble those observed in Jupiter's post-dusk polar cusp region as reported by Xu et al. (2024) (see Supplementary Note 1), indicating a consistent cusp microphysics and complex magnetosphric structures across different giant planets.

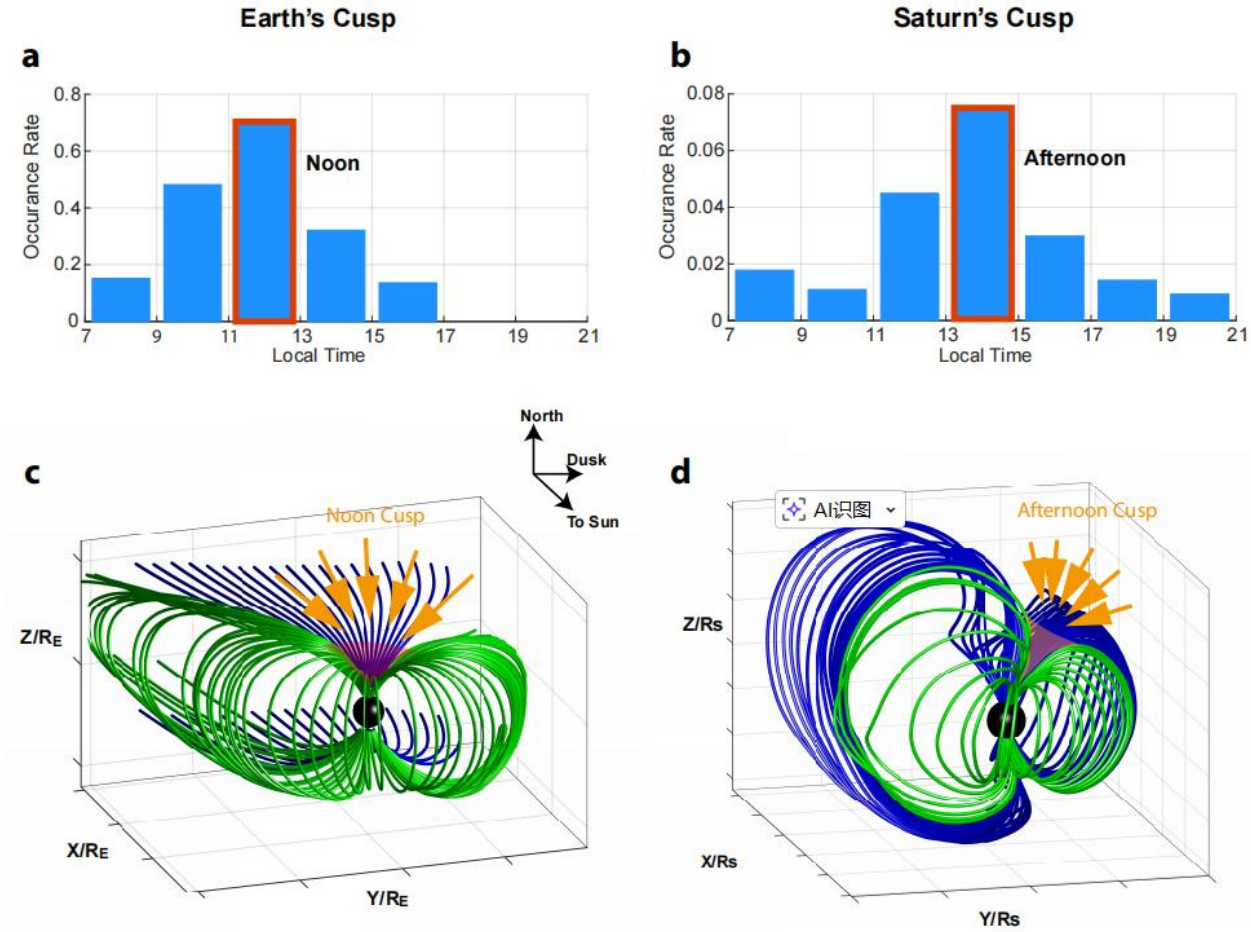

Figure 4. Occurrence rate distributions of Earth's and Saturn's cusp revealed by in situ data and magnetic field configurations of Earth and Saturn, as demonstrated by high-resolution simulations. (a) Occurrence rate distributions of Earth's cusp under magnetic local time detected by Cluster datasets using the same time range in Zhang et al.'s statistical work[52] and of (b) Saturn's cusp detected by Cassini datasets. A general visual representation of

magnetic configurations near the magnetopause of (c) Earth and (d) Saturn exhibited by MHD simulation. The simulation results for Earth in Fig. 4c are from Chen et al. (2023)[12]. The green field lines represent the magnetic field structures near the day side, while the blue lines indicate those near the night side. In Earth's magnetic field configuration, the blue line specifically denotes the open lobe structure. The magnetic field lines shown for Saturn are all closed field lines.

To quantify this asymmetry, we computed the probability distribution of the cusp with the time resolution of 1 minute, as depicted in Fig. 4b. Additionally, for comparative purposes with Saturn, we replicated Earth's cusp probability distribution using the Cluster electron and magnetic field datasets[52] as shown in Fig. 4a. Noted that the Cusp detections at different local times are normalized by the spacecraft's high-latitude dwell time at corresponding local times for both Cluster and Cassini, minimizing potential statistical biases caused by orbital differences. For detailed information on event identification and case presentations in Earth's cusp region, please refer to Supplementary Note 2 and Supplementary Fig. 4. The results of this distribution are consistent with previous studies[20]: The peak occurrence rate of Earth's cusp is centered around noon (11-13 LT), with some disparity between the morning and afternoon sides, which can be attributed to the influence of the IMF B_y component and solar wind dynamic pressure, which can shift and modify the cusp's position during spacecraft observation[22,23]. In contrast, the peak occurrence rate of Saturn's cusp manifests on the afternoon side 13-15 LT. Notably, Saturn's cusp distribution does not mirror the shift of Earth's cusp distribution toward the afternoon under positive IMF B_y condition[22]. Instead, it shows a clear shift in overall distribution toward the dusk or even night side. Global MHD simulations[11,29,44], as illustrated in Figs. 4c and

4d, map the magnetic field configurations near the magnetopauses of Earth and Saturn, highlighting the differences between their distributions. Saturn's magnetopause, influenced by the planet's rapid rotational dynamics, is more expanded on the morning side compared to the afternoon side, in agreement with previous MHD simulations and observations which found the magnetopause was typically expanded by 1-2 R_s on the dawnside compared to dusk[41,53,54]. The cusp must conform to this topology, leading to the observed asymmetry and enabling cusp observations even on the post-dusk side—an occurrence hardly seen at Earth[20,22]. Moreover, the simulation results reveal Saturn's magnetopause reconnection picture under typical solar wind conditions, which closely resembles that of Jupiter[12,13]. Reconnection occurs predominantly at high latitudes and is suppressed at low-latitude magnetopause regions—distinct from Earth, where reconnection is primarily governed by the north–south component of the interplanetary magnetic field[7,14,55]. For a detailed presentation and analysis of Saturn's magnetopause reconnection results, please refer to Supplementary Note 3 and Supplementary Figs. 5–6.

Discussion

Our global analysis of Saturn's magnetospheric cusps, supplemented by high-resolution global MHD simulations, has led to several helpful insights that expand our understanding of planetary magnetospheres. The result shows a marked dawn-dusk asymmetry in Saturn's cusp distribution, in strong contrast to Earth's symmetrical cusp structure. Cassini spacecraft observations reveal that Saturn's cusps are not uniformly distributed around the noon sector but are predominantly located in the post-noon region, with cusp structures extending into the post-dusk sector (near 20 LT). In other words, the overall spatial distribution of Saturn's cusp is shifted toward the dusk side, a feature driven by the rapid rotation–induced magnetospheric dynamics characteristic of giant planets. This finding provides key observational evidence that complements recent reports

of Jupiter's dusk-side cusp regions[13] and marks a advance in understanding the complex global magnetospheric topology of giant planets.

Furthermore, our high-resolution simulations reveal that Saturn's magnetopause magnetic topology closely resembles the recently reported simulated configuration at Jupiter[11–13]. Compared with previous simulation studies that identified asymmetries at Saturn's magnetopause[41], the results presented here provide a more detailed and comprehensive global view of the magnetopause structure. This structure is characterized by a more expanded geometry on the dawn side than on the dusk side and features stronger east–west magnetic components and potential increased sensitivity to the east–west component of the IMF. Under typical B_y-dominated solar wind conditions around 5 and 10 AU[56,57], resulting Saturn's magnetopause reconnection pattern mirrors that of Jupiter, with reconnection occurring predominantly at high latitudes (see Supplementary Note 3). It is not fully clear how the rapid rotation-driven magnetospheric dynamics causes the magnetospheric morning-afternoon asymmetry, but the global MHD simulations can provide some insightful clues and be instrumental in understanding the underlying dynamics that contribute to this asymmetry.

Numerical simulations by Zhang et al.[29] indicate closed magnetic flux accumulation picture in the pre-noon sector at Saturn. Saturn's rapid rotation drives a rotation-dominated transport of closed magnetic flux toward the dayside magnetosphere. Concurrently, the counterclockwise flux transport on the dawn side opposes the direction of the incoming solar wind, while the magnetopause boundary restricts the noonward migration of flux tubes due to low magnetopause reconnection rates. Consequently, closed magnetic flux significantly accumulates in the pre-noon sector (as shown in Supplementary Fig. 7), which might significantly alter the open-closed boundary configuration of Saturn's magnetosphere. The resulting flux pileup in the pre-noon

sector increases the local magnetic pressure near the dawn magnetopause, causing the boundary to expand outward balancing with the solar wind's ram pressure. This produces an expanded magnetospheric configuration on the morning side compared to the afternoon side—an asymmetry consistent with previous Jupiter[12] and Saturn[41] simulation results. Since the cusp is inherently anchored to this topology, its global distribution exhibits a duskward bias.

Furthermore, the cusp distribution revealed in this study shows that nearly all features shift duskward (even nightside) from the noon side, rather than equally towards dawn and dusk as observed at Earth. This duskward observation aligns with the lagging field configuration at Saturn ($B_\varphi < 0$ in the northern hemisphere). This suggests another effect of rapid rotation could be the continued motion of newly-opened field lines (flux tubes) in the duskward direction. The ion dispersions analyzed by Arridge et al.[40] indicate transit times from the reconnection site of 1-10 hours. Given a polar cap subcorotating at 30% of the corotation rate[58], the field line can move 10-120 degrees (about 1-8 hours LT) azimuthally duskward before the plasma is detected by the spacecraft. Consequently, magnetopause reconnection signatures (ion dispersion, magnetosheath-like electrons) used to identify the cusp will be more commonly observed towards dusk, which has been implicit by models and observations from previous studies[33,34,59].

Prior research has noted parallels in the properties of charged particles among Jupiter's, Saturn's, and Earth's cusp[13,37,40,60]. This implies that although the macroscopic positioning of the cusps may differ owing to planet-specific factors, such as rotation speed, internal plasma sources, and scale sizes compared with convection, the microphysical processes that dictate the behavior of charged particles within the cusps might be consistent across varied planetary environments.

In summary, our study contributes helpful insights into planetary magnetospheres. The identification of dawn-dusk asymmetry in Saturn's cusp distribution, including evidence of post-

dusk cusp observations, implys the influence of a rapidly rotating magnetosphere with internal particle sources on the overall magnetospheric configuration. Furthermore, our high-resolution simulations reveal that Saturn's magnetopause magnetic topology and magnetopause reconnection pattern closely resemble the recently identified configuration at Jupiter. This provides evidence for a shared physical mechanism governing solar wind interaction at rapidly rotating giant planets—one that fundamentally differs from Earth's magnetopause coupling processes. This finding broadens our understanding of planetary interactions with the solar winds. Such insights offer helpful guidance for future exploration of magnetospheric boundaries and cusp regions at giant planets both within and beyond our solar system. They can help formulate more precise models of planetary magnetospheres, providing a complementary perspective for analyzing the complex interactions between planetary magnetic fields and the solar wind.

Methods

Simulation Information

In this study, the global MHD model of Saturn's magnetic configuration (Fig. 4d) is built upon the GAMERA code (Grid Agnostic MHD for Extended Research Applications) to tackle equations on a specifically designed curvilinear, non-orthogonal grid suited for the study of planetary magnetospheres[44]. The computational model employs a grid of 256 × 256 × 256 cells, and the grid implemented in this model is a nonuniform, distorted spherical grid, oriented along the Solar Magnetic (SM) X-axis and possessing a symmetry axis. The grid exhibits non-uniformity in the radial-azimuthal plane, with cell sizes reducing as they approach Saturn. The simulation begins at an inner boundary of 4 R_S, with boundary conditions obtained from electrostatic potential models[61,62]. The outer boundary takes the form of a cylinder, stretching

from SM-X = 56 R_s to SM-X = -600 R_s, with a radius around 214 R_s. The conditions at this outer boundary are controlled by the solar wind and the interplanetary magnetic field (IMF). The grid is structured so that its resolution diminishes with increasing distance from Saturn, which enhances computational efficiency by aligning with the larger scale of magnetospheric processes farther from the planet. The radial cell sizes near Saturn's magnetopause range between approximately 0.1 and 0.2 R_s. This model is driven by simplified representations of solar wind and IMF conditions, setting IMF B_z at -0.5 nT, a particle density of 0.1 per cubic centimeter, a solar wind velocity of 400 km/s, and a solar wind pressure of 2.8×10^{-5} nPa. The dipole tilt of Saturn's magnetic field is maintained at 0 degrees to remove hemispheric asymmetries, thereby simplifying the overall analysis. Moreover, the moon Enceladus ejects plasma into Saturn's magnetosphere[63,64], creating an internal plasma source that migrates outward and influences the magnetopause. The simulation data presented in this paper are publicly available online via Xu (2026)[65].

Cassini and Cluster Data

We analyzed magnetometer (MAG), electron spectrometer (ELS), and ion mass spectrometer (IMS) data from the Cassini spacecraft spanning 2004-2010. Data were obtained from the NASA Planetary Data System. We analyzed magnetic field observations and position data from the Cassini MAG instrument[45], and thermal ion and electron measurements with energy ranges up to 28 keV (electrons) and 50 keV (ions) from Cassini-CAPS/IMS/ELS[46]. Cluster magnetic field and particle data were obtained from the ESA Cluster Science Archive. The data sets to analyze Earth's cusp were obtained by the FGM[66], PEACE[67], CIS[68], and WHISPER[69] instruments onboard Cluster. Detailed identification information of Earth’s cusp is shown in Supplementary Note 2.

Data availability

All Cassini data presented here are publicly available from NASA's Planetary Data System (https://pds-ppi.igpp.ucla.edu/). The MAG dataset of Cassini is available via https://search-pdsppi.igpp.ucla.edu/search/view/?f=yes&id=pds://PPI/cassini-mag-cal. The CAPS dataset of Cassini is available via https://search-pdsppi.igpp.ucla.edu/search/?sc=Cassini&i=CAPS. The Cluster data used in this paper can be obtained from the Cluster Science Archive via https://csa.esac.esa.int/csa-web/. The simulation data of Saturn's magnetospheric topology presented in this paper are publicly available online via Xu (2026)[65] https://doi.org/10.17605/OSF.IO/RQJYH. The datasets generated during and/or analysed during the current study are available from the corresponding author upon request.

Code availability

The Cassini data are processed and analyzed using the Spedas package[70], which can be downloaded via the https://github.com/spedas page. The presentation of simulated data can be done by any standard plotting codes (Python/Matlab), for example, the Python function matplotlib.integrate (which can be downloaded via the https://matplotlib.org/stable/install/ page). The Matlab code used in the analysis of simulations is publicly available online via Xu (2026)[65] https://doi.org/10.17605/OSF.IO/RQJYH.

References

1. Kivelson, M. G. & Southwood, D. J. Dynamical consequences of two modes of centrifugal instability in Jupiter's outer magnetosphere. *Journal of Geophysical Research: Space Physics* **110**, (2005).
2. Delamere, P. A., Otto, A., Ma, X., Bagenal, F. & Wilson, R. J. Magnetic flux circulation in the rotationally driven giant magnetospheres. *Journal of Geophysical Research: Space Physics* **120**, 4229–4245 (2015).

3. Lepping, R. P. Comparisons of the field configurations of the magnetotails of Uranus and Neptune. *Planetary and Space Science* **42**, 847–857 (1994).
4. Jasinski, J. M., Murphy, N., Jia, X. & Slavin, J. A. Neptune's Pole-on Magnetosphere: Dayside Reconnection Observations by Voyager 2. *Planet. Sci. J.* **3**, 76 (2022).
5. Cowley, S. W. H., Bunce, E. J., Stallard, T. S. & Miller, S. Jupiter's polar ionospheric flows: Theoretical interpretation. *Geophysical Research Letters* **30**, (2003).
6. Cowley, S. W. H., Badman, S. V., Imber, S. M. & Milan, S. E. Comment on "Jupiter: A fundamentally different magnetospheric interaction with the solar wind" by D. J. McComas and F. Bagenal. *Geophysical Research Letters* **35**, (2008).
7. Dungey, J. W. Interplanetary magnetic field and the auroral zones. *Physical review letters* **6**, 47 (1961).
8. Fuselier, S. A. *et al.* The location of magnetic reconnection at Saturn's magnetopause: A comparison with Earth. *Journal of Geophysical Research: Space Physics* **119**, 2563–2578 (2014).
9. Montgomery, J. *et al.* Investigating the Occurrence of Magnetic Reconnection at Jupiter's Dawn Magnetopause During the Juno Era. *Geophysical Research Letters* **49**, e2022GL099141 (2022).
10. Fuselier, S. A., Petrinec, S. M., Sawyer, R. P., Mukherjee, J. & Masters, A. Suppression of Magnetic Reconnection at Saturn's Low-Latitude Magnetopause. *Journal of Geophysical Research: Space Physics* **125**, e2020JA027895 (2020).
11. Zhang, B. *et al.* How Jupiter's unusual magnetospheric topology structures its aurora. *Science Advances* **7**, eabd1204 (2021).
12. Chen, J. *et al.* Prediction of Axial Asymmetry in Jovian Magnetopause Reconnection. *Geophysical Research Letters* **50**, e2022GL102577 (2023).
13. Xu, Y. *et al.* In situ evidence of the magnetospheric cusp of Jupiter from Juno spacecraft measurements. *Nat Commun* **15**, 6062 (2024).
14. Cargill, P. J. *et al.* Cluster at the Magnetospheric Cusps. *Space Sci Rev* **118**, 321–366 (2005).
15. Russell, C. T. The polar cusp. *Advances in Space Research* **25**, 1413–1424 (2000).
16. Kistler, L. M., Mouikis, C. G., Klecker, B. & Dandouras, I. Cusp as a source for oxygen in the plasma sheet during geomagnetic storms. *Journal of Geophysical Research: Space Physics* **115**, (2010).

17. Vogiatzis, I. I. *et al.* Cluster observations of particle acceleration up to supra-thermal energies in the cusp region related to low-frequency wave activity - possible implications for the substorm initiation process. *Annales Geophysicae* **26**, 653–669 (2008).
18. Fuselier, S. A., Frey, H. U., Trattner, K. J., Mende, S. B. & Burch, J. L. Cusp aurora dependence on interplanetary magnetic field Bz. *Journal of Geophysical Research: Space Physics* **107**, SIA 6-1-SIA 6-10 (2002).
19. Smith, M. F. & Lockwood, M. Earth's magnetospheric cusps. *Reviews of Geophysics* **34**, 233–260 (1996).
20. Newell, P. T. & Meng, C.-I. The cusp and the cleft/boundary layer: Low-altitude identification and statistical local time variation. *Journal of Geophysical Research: Space Physics* **93**, 14549–14556 (1988).
21. Měrka, J., Šafránková, J. & Němeček, Z. Cusp-like plasma in high altitudes: a statistical study of the width and location of the cusp from Magion-4. *Annales Geophysicae* **20**, 311–320 (2002).
22. Newell, P. T., Meng, C.-I., Sibeck, D. G. & Lepping, R. Some low-altitude cusp dependencies on the interplanetary magnetic field. *Journal of Geophysical Research: Space Physics* **94**, 8921–8927 (1989).
23. Lundin, R., Aparicio, B. & Yamauchi, M. On the solar wind flow control of the polar cusp. *Journal of Geophysical Research: Space Physics* **106**, 13023–13035 (2001).
24. Wilson, R. J. *et al.* Cassini plasma spectrometer thermal ion measurements in Saturn's inner magnetosphere. *Journal of Geophysical Research: Space Physics* **113**, (2008).
25. Kane, M., Mitchell, D. G., Carbary, J. F., Krimigis, S. M. & Crary, F. J. Plasma convection in Saturn's outer magnetosphere determined from ions detected by the Cassini INCA experiment. *Geophysical Research Letters* **35**, (2008).
26. Greathouse, T. *et al.* Local Time Dependence of Jupiter's Polar Auroral Emissions Observed by Juno UVS. *Journal of Geophysical Research: Planets* **126**, e2021JE006954 (2021).
27. Grodent, D., Gérard, J.-C., Cowley, S. W. H., Bunce, E. J. & Clarke, J. T. Variable morphology of Saturn's southern ultraviolet aurora. *Journal of Geophysical Research: Space Physics* **110**, (2005).
28. Yao, Z. H. *et al.* Corotating Magnetic Reconnection Site in Saturn's Magnetosphere. *The Astrophysical Journal Letters* **846**, L25 (2017).
29. Zhang, B. *et al.* A unified framework for global auroral morphologies of different planets. *Nat Astron* **8**, 964–972 (2024).

30. Gombosi, T. I. *et al.* Saturn's Magnetospheric Configuration. in *Saturn from Cassini-Huygens* (eds Dougherty, M. K., Esposito, L. W. & Krimigis, S. M.) 203–255 (Springer Netherlands, Dordrecht, 2009). doi:10.1007/978-1-4020-9217-6_9.
31. Jinks, S. L. *et al.* Cassini multi-instrument assessment of Saturn's polar cap boundary. *Journal of Geophysical Research: Space Physics* **119**, 8161–8177 (2014).
32. Jasinski, J. M. *et al.* Saturn's Open-Closed Field Line Boundary: A Cassini Electron Survey at Saturn's Magnetosphere. *Journal of Geophysical Research: Space Physics* **124**, 10018–10035 (2019).
33. Cowley, S. W. H., Bunce, E. J. & O'Rourke, J. M. A simple quantitative model of plasma flows and currents in Saturn's polar ionosphere. *Journal of Geophysical Research: Space Physics* **109**, (2004).
34. Cowley, S. W. H. *et al.* Reconnection in a rotation-dominated magnetosphere and its relation to Saturn's auroral dynamics. *Journal of Geophysical Research: Space Physics* **110**, (2005).
35. Vasyliunas, V. M. Plasma distribution and flow. in *Physics of the Jovian Magnetosphere* (ed. Dessler, A. J.) 395–453 (Cambridge University Press, Cambridge, 1983). doi:10.1017/CBO9780511564574.013.
36. Arridge, C. S., Kane, M., Sergis, N., Khurana, K. K. & Jackman, C. M. Sources of Local Time Asymmetries in Magnetodiscs. in *The Magnetodiscs and Aurorae of Giant Planets* (eds Szego, K. et al.) 301–333 (Springer, New York, NY, 2016). doi:10.1007/978-1-4939-3395-2_8.
37. Jasinski, J. M. *et al.* Cusp observation at Saturn's high-latitude magnetosphere by the Cassini spacecraft. *Geophysical Research Letters* **41**, 1382–1388 (2014).
38. Jasinski, J. M. *et al.* Cassini plasma observations of Saturn's magnetospheric cusp. *Journal of Geophysical Research: Space Physics* **121**, 12,047-12,067 (2016).
39. Jasinski, J. M. *et al.* Diamagnetic depression observations at Saturn's magnetospheric cusp by the Cassini spacecraft. *Journal of Geophysical Research: Space Physics* **122**, 6283–6303 (2017).
40. Arridge, C. S. *et al.* Cassini observations of Saturn's southern polar cusp. *Journal of Geophysical Research: Space Physics* **121**, 3006–3030 (2016).
41. Jia, X. & Kivelson, M. G. Dawn-dusk asymmetries in rotating magnetospheres: Lessons from modeling Saturn. *Journal of Geophysical Research: Space Physics* **121**, 1413–1424 (2016).
42. Bolton, S. J. *et al.* The Juno Mission. *Space Sci Rev* **213**, 5–37 (2017).

43. Lund, T. Juno Spacecraft. in *Spacecraft Exploring Outer Planets: From Jupiter to Neptune* (ed. Lund, T.) 259–299 (Springer Nature Switzerland, Cham, 2025). doi:10.1007/978-3-031-96544-9_9.
44. Zhang, B. *et al.* GAMERA: A Three-dimensional Finite-volume MHD Solver for Non-orthogonal Curvilinear Geometries. *ApJS* **244**, 20 (2019).
45. Dougherty, M. K. *et al.* The Cassini Magnetic Field Investigation. in *The Cassini-Huygens Mission: Orbiter In Situ Investigations Volume 2* (ed. Russell, C. T.) 331–383 (Springer Netherlands, Dordrecht, 2004). doi:10.1007/978-1-4020-2774-1_4.
46. Young, D. T. *et al.* Cassini Plasma Spectrometer Investigation. *Space Science Reviews* **114**, 1–112 (2004).
47. Thomsen, M. F. *et al.* Survey of Magnetosheath Plasma Properties at Saturn and Inference of Upstream Flow Conditions. *Journal of Geophysical Research: Space Physics* **123**, 2034–2053 (2018).
48. Lockwood, M. & Smith, M. F. Low and middle altitude cusp particle signatures for general magnetopause reconnection rate variations: 1. Theory. *Journal of Geophysical Research: Space Physics* **99**, 8531–8553 (1994).
49. Zieger, B. & Hansen, K. C. Statistical validation of a solar wind propagation model from 1 to 10 AU. *Journal of Geophysical Research: Space Physics* **113**, (2008).
50. Gurnett, D. A. *et al.* Discovery of a north-south asymmetry in Saturn's radio rotation period. *Geophysical Research Letters* **36**, L16102 (2009).
51. Nakamura, Y. *et al.* Seasonal variation of north–south asymmetry in the intensity of Saturn Kilometric Radiation from 2004 to 2017. *Planetary and Space Science* **178**, 104711 (2019).
52. Zhang, H., Fritz, T. A., Zong, Q.-G. & Daly, P. W. Stagnant exterior cusp region as viewed by energetic electrons and ions: A statistical study using Cluster Research with Adaptive Particle Imaging Detectors (RAPID) data. *Journal of Geophysical Research: Space Physics* **110**, (2005).
53. Kivelson, M. G. & Jia, X. Control of periodic variations in Saturn's magnetosphere by compressional waves. *Journal of Geophysical Research: Space Physics* **119**, 8030–8045 (2014).
54. Pilkington, N. M. *et al.* Asymmetries observed in Saturn's magnetopause geometry. *Geophysical Research Letters* **42**, 6890–6898 (2015).
55. Pitout, F., Escoubet, C. P., Klecker, B. & Rème, H. Cluster survey of the mid-altitude cusp: 1. size, location, and dynamics. *Annales Geophysicae* **24**, 3011–3026 (2006).

56. Ebert, R. W., Bagenal, F., McComas, D. J. & Fowler, C. M. A survey of solar wind conditions at 5 AU: a tool for interpreting solar wind-magnetosphere interactions at Jupiter. *Front. Astron. Space Sci.* **1**, (2014).
57. Achilleos, N. *et al.* Large-scale dynamics of Saturn's magnetopause: Observations by Cassini. *Journal of Geophysical Research: Space Physics* **113**, (2008).
58. Stallard, T. S., Miller, S., Trafton, L. M., Geballe, T. R. & Joseph, R. D. Ion winds in Saturn's southern auroral/polar region. *Icarus* **167**, 204–211 (2004).
59. Bunce, E. J., Cowley, S. W. H. & Milan, S. E. Interplanetary magnetic field control of Saturn's polar cusp aurora. *Annales Geophysicae* **23**, 1405–1431 (2005).
60. Zong, Q.-G. *et al.* Multiple cusps during an extended northward IMF period with a significant By component. *Journal of Geophysical Research: Space Physics* **113**, (2008).
61. Lyon, J. G., Fedder, J. A. & Mobarry, C. M. The Lyon–Fedder–Mobarry (LFM) global MHD magnetospheric simulation code. *Journal of Atmospheric and Solar-Terrestrial Physics* **66**, 1333–1350 (2004).
62. Merkin, V. G. & Lyon, J. G. Effects of the low-latitude ionospheric boundary condition on the global magnetosphere. *Journal of Geophysical Research: Space Physics* **115**, (2010).
63. Haff, P. K., Eviatar, A. & Siscoe, G. L. Ring and plasma: The enigmae of Enceladus. *Icarus* **56**, 426–438 (1983).
64. Bagenal, F. & Delamere, P. A. Flow of mass and energy in the magnetospheres of Jupiter and Saturn. *Journal of Geophysical Research: Space Physics* **116**, (2011).
65. Xu, Y. Simulation Dataset for "Dawn-dusk Asymmetrical Distribution of Saturn's Cusp". The Open Science Framework (2026) doi:10.17605/OSF.IO/RQJYH.
66. Balogh, A. *et al.* THE CLUSTER MAGNETIC FIELD INVESTIGATION. *Space Science Reviews* **79**, 65–91 (1997).
67. Johnstone, A. D. *et al.* Peace: A Plasma Electron and Current Experiment. in *The Cluster and Phoenix Missions* (eds Escoubet, C. P., Russell, C. T. & Schmidt, R.) 351–398 (Springer Netherlands, Dordrecht, 1997). doi:10.1007/978-94-011-5666-0_13.
68. Rème, H. *et al.* The Cluster Ion Spectrometry (CIS) Experiment. in *The Cluster and Phoenix Missions* (eds Escoubet, C. P., Russell, C. T. & Schmidt, R.) 303–350 (Springer Netherlands, Dordrecht, 1997). doi:10.1007/978-94-011-5666-0_12.

69. Décréau, P. M. E. *et al.* WHISPER, A RESONANCE SOUNDER AND WAVE ANALYSER: PERFORMANCES AND PERSPECTIVES FOR THE CLUSTER MISSION. *Space Science Reviews* **79**, 157–193 (1997).
70. Angelopoulos, V. *et al.* The Space Physics Environment Data Analysis System (SPEDAS). *Space Sci Rev* **215**, 9 (2019).

Acknowledgement

This work was supported by the National Natural Science Foundation of China (NSFC) grants 42508013 (Y.X.), 42374212 (Z.Y.), 42374216 (B.Z.), and 42274221 (S.Y.); the China Postdoctoral Science Foundation (CPSF) grant 2025M770390 (Y.X.) and the Postdoctoral Fellowship Program of CPSF grant GZB20250099 (Y.X.); the Research Grants Council (RGC) General Research Fund grants 17309124 (Z.Y.), 17308221 (B.Z.), 17315222 (B.Z.), and 17308723 (B.Z.); the Hong Kong RGC Co-funding Mechanism on Joint Laboratories with the Chinese Academy of Sciences project JLFS/P-702/24 (Z. Y.); UCL-MSSL STFC consolidated Grant ST/W001004/1 (A. J. C.); STFC Grant ST/Y002148/1 to Lancaster University (L. C. R); UKRI STFC grant ST/Y002393/1 (S. V. B.).

Author contributions

Z. H. Y. proposed the original framework for the work. Y. X. conceived the specific research methodologies, refined the initial framework, carried out data analyses, drew all figures and wrote the initial draft. C. S. A. provided overall guidance for data analyses and research methodologies. B. Z. prepared the data of Fig. 4d and contributed images and tools for the representation of Saturn's magnetospheric configuration. J. J. C. helped in understanding the

picture of magnetic configuration related to Saturn's cusp, providing figures and datasets of Earth's simulated magnetic configuration. S. V. B. and L. C. R. provided guidance and assistance in data analyses and discussing magnetospheric picture. A. J. C. provided guidance and assistance in discussion and provided magnetic field data from Cassini, as well as data from Plasma Spectrometer instruments. Y. X., Z. H. Y., C. S. A., L. C. R., S. V. B., S. Y. Y., W. R. D., Z. Q. Z., Y. W., and T. S. Q. contributed to manuscript revisions and interpretation of results.

Competing interests

The authors declare no competing interests.